Quantal nucleon diffusion: Central collisions of symmetric nuclei

S. Ayik,[1,*] O. Yilmaz,[2] B. Yilmaz,[3] and A. S. Umar[4]

[1]*Physics Department, Tennessee Technological University, Cookeville, Tennessee 38505, USA*
[2]*Physics Department, Middle East Technical University, 06800 Ankara, Turkey*
[3]*Physics Department, Faculty of Sciences, Ankara University, 06100 Ankara, Turkey*
[4]*Department of Physics and Astronomy, Vanderbilt University, Nashville, Tennessee 37235, USA*

The quantal diffusion mechanism of nucleon exchange is studied in the central collisions of several symmetric heavy ions in the framework of the stochastic mean-field (SMF) approach. Since, at bombarding energies below the fusion barrier, dinuclear structure is maintained, it is possible to describe nucleon exchange as a diffusion process familiar from deep-inelastic collisions. Quantal diffusion coefficients, including memory effects, for proton and neutron exchanges are extracted microscopically employing the SMF approach. The quantal calculations of neutron and proton variances are compared with the semiclassical results.

I. INTRODUCTION

Multinucleon exchange is an important mechanism in deep-inelastic heavy-ion collisions. Considerable effort has been spent to describe deep-inelastic collisions in terms of nucleon transport models [1–4]. More recently, it has been realized that multinucleon exchange is an important process in the quasifission reactions of heavy ions [5]. The challenge of nuclear theory, for these reactions, is to describe the entrance channel dynamics leading either to fusion or to quasifission, as well as the dynamical evolution of the dinuclear complex toward a compound nucleus [6–10]. Dynamical description of the reaction mechanisms is often done within macroscopic or microscopic-macroscopic approaches [11–16]. A mean-field approach such as the time-dependent Hartree-Fock (TDHF) theory provides a microscopic basis for describing the heavy-ion reaction mechanism at low bombarding energies [17,18]. For heavy systems, at collision energies near the fusion barrier, the compound nucleus formation is severely inhibited by the quasifission mechanism. The colliding ions stick together for a long time, but separate without going through the compound nucleus formation. During the long contact times many nucleons are exchanged between the projectile and the target nuclei. In multinucleon exchange reactions, it is possible to study charge equilibration driven by the nuclear symmetry energy [19], and to produce very neutron-rich heavy ions [20,21]. A number of models have been developed for the description of the reaction mechanism in the multinucleon transfer process in quasifission reactions [7,13,22,23]. Within the last few years the TDHF approach has been utilized to study the dynamics of quasifission [24–27]. Particularly, the study of quasifission is showing great promise to provide insight based on very favorable comparisons with experimental data. However, in the mean-field approximation the collective aspects of collision dynamics are treated semiclassically, and fluctuations of the macroscopic variables are severely inhibited. To remedy this problem one must go beyond TDHF [28–30].

In the recently developed stochastic mean-field (SMF) approach, the dynamical description is extended beyond the mean-field approximation by incorporating the initial fluctuations [30,31]. In a number of studies, it has been demonstrated that the SMF approach alleviates the drawbacks of the standard mean-field approach and improves the description of nuclear collision dynamics by including the fluctuation mechanism of the collective motion [30,32–37]. Most applications have been carried out for collisions where a dinuclear structure is maintained. In this case it is possible to define macroscopic variables by a geometric projection procedure with the help of the window dynamics. The SMF approach gives rise to a Langevin description for the evolution of macroscopic variables [38,39]. In most analyses of the nucleon diffusion mechanism, the deduced Langevin description has been applied by calculating transport coefficients in the semiclassical approximation and neglecting the memory effects. In a recent work, we investigated nucleon exchange mechanism for the central collisions of several symmetric systems in the quantal framework of the SMF approach under a certain approximation [40]. In this work, we consider central collisions of symmetric systems below the fusion barrier as well, but improve the quantal description of the diffusion mechanism to a large extent. We extract quantal diffusion coefficients for proton and neutron transfers, including memory effects, from the SMF approach. In symmetric collisions, the mean values of the proton and neutron numbers of the outgoing fragments do not change. However, as result of nucleon exchange, outgoing fragments exhibit charge and mass distributions around their initial values. We carry out calculations for the variance of neutron and proton distributions of the outgoing fragments in the central collisions of $^{28}O+^{28}O$, $^{40}Ca+^{40}Ca$, $^{48}Ca+^{48}Ca$, and $^{56}Ni+^{56}Ni$ systems at bombarding energies slightly below their fusion barriers, and compare the results with the corresponding semiclassical calculations.

In Sec. II, we present a brief description of the quantal nucleon diffusion mechanism based on the SMF approach. In Sec. III, we present a derivation of the quantal expression for proton and neutron diffusion coefficients. The result of calculations is reported in Sec. IV, and conclusions are given in Sec. V.

*ayik@tntech.edu

044624-1

II. DIFFUSION MECHANISM

In heavy-ion collisions, when the system maintains a binary structure, the reaction evolves primarily by nucleon exchange through the window between the projectile-like and target-like fragments. It is possible to analyze the nucleon exchange mechanism by employing a nucleon diffusion concept based on the SMF approach. In the SMF approach, the standard mean-field description is extended by incorporating the mean-field fluctuations in terms of generating an ensemble of events according to quantal and thermal fluctuations in the initial state. Instead of following a single event specified by fixed initial conditions, in the SMF approach an ensemble of events are propagated specified in terms of the quantal and thermal fluctuations of the initial state; for details please refer to [31–36]. In extracting transport coefficients for nucleon exchange, we take the proton and neutron numbers of projectile-like fragments Z_1^λ, N_1^λ as independent variables, where λ indicates the event label. We can define the proton and neutron numbers of the projectile-like fragments in each event by integrating over the nucleon density on the projectile side of the window. In central collisions of symmetric systems, the window is perpendicular to the collision direction, taken as the x axis, and the position of the window is fixed at the origin of the center-of-mass frame at $x_0 = 0$. The proton and neutron numbers of the projectile-like fragments are defined as

$$\begin{pmatrix} Z_1^\lambda(t) \\ N_1^\lambda(t) \end{pmatrix} = \int d^3r \, \theta(x - x_0) \begin{pmatrix} \rho_p^\lambda(\vec{r},t) \\ \rho_n^\lambda(\vec{r},t) \end{pmatrix}. \qquad (1)$$

Here, $\rho_p^\lambda(\vec{r},t)$ and $\rho_n^\lambda(\vec{r},t)$ are the local densities of protons and neutrons, and $x_0 = 0$. According to the SMF approach, the proton and neutron numbers of the projectile-like fragment follow a stochastic evolution according to the Langevin equations,

$$\frac{d}{dt} \begin{pmatrix} Z_1^\lambda(t) \\ N_1^\lambda(t) \end{pmatrix} = \int d^3r \, g(x) \begin{pmatrix} J_{x,p}^\lambda(\vec{r},t) \\ J_{x,n}^\lambda(\vec{r},t) \end{pmatrix} = \begin{pmatrix} v_p^\lambda(t) \\ v_n^\lambda(t) \end{pmatrix}. \quad (2)$$

In this expression, we introduce a smoothing function $g(x)$ for convenience:

$$g(x) = \frac{1}{\sqrt{2\pi}\kappa} \exp\left(-\frac{x^2}{2\kappa^2}\right). \qquad (3)$$

In the limit $\kappa \to 0$, $g(x)$ becomes a delta function $g(x) \to \delta(x)$. The right-hand side of Eq. (2) denotes the proton, $v_p^\lambda(t)$, and neutron, $v_n^\lambda(t)$, drift coefficients for the event λ, which are determined by the proton and the neutron current densities, $J_{x,p}^\lambda(\vec{r},t), J_{x,n}^\lambda(\vec{r},t)$, through the window for that event. In the SMF approach, the fluctuating proton and neutron current densities are defined as

$$J_{x,\alpha}^\lambda(\vec{r},t) = \frac{\hbar}{m} \sum_{ij\in\alpha} \text{Im}\left[\Phi_j^*(\vec{r},t;\lambda) \nabla_x \Phi_i(\vec{r},t;\lambda) \rho_{ji}^\lambda\right]. \quad (4)$$

Here, and in the rest of the paper, we use the label $\alpha = p, n$ for the proton and neutron states. The parameter κ of the Gaussian smoothing function is determined by setting typical particle-hole matrix elements of proton and neutron currents

through the window

$$\Lambda_{ji}^\lambda(t) = \int d^3r \, g(x) \, \text{Im}[\Phi_j^*(\vec{r},t;\lambda) \nabla_x \Phi_i(\vec{r},t;\lambda)] \qquad (5)$$

to their values obtained at $\kappa \to 0$ as $g(x) \to \delta(x)$. It turns out that this limiting value equals the smoothed value by means of a Gaussian with a dispersion given by value $\kappa = 1.0$ fm. This value is on the order of lattice spacing, which indicates the numerical calculations implicitly involve such a smoothing mechanism. Drift coefficients fluctuate from event to event due to stochastic elements of the initial density matrix ρ_{ji}^λ and also due to the different sets of the wave functions in different events. As a result, there are two sources for fluctuations of the nucleon current: (i) fluctuations arising from the state dependence of the drift coefficients, which may be approximately represented in terms of fluctuations of proton and neutron numbers of the dinuclear system, and (ii) the explicit fluctuations $\delta v_p^\lambda(t)$ and $\delta v_n^\lambda(t)$, which arise from the stochastic part of the proton and neutron currents [29,36]. In the present work, we investigate the nucleon diffusion mechanism for the central collisions of light heavy ions. Due to the relatively short collision times, fluctuations driven by the symmetry energy are small. Therefore, we neglect the fluctuation mechanism due to the state dependence of the drift coefficients and include only the explicit fluctuations arising from the stochastic part of the current densities. Equations for the mean values of proton, $Z_1(t) = \overline{Z_1^\lambda(t)}$, and neutron, $N_1(t) = \overline{N_1^\lambda(t)}$, numbers of the projectile-like fragments are obtained by taking the ensemble averaging of the Langevin equation (2). Here and below, the bar over a quantity indicates the average over the generated ensemble. For small amplitude fluctuations, we obtain the usual mean-field result given by the TDHF equations,

$$\frac{d}{dt} \begin{pmatrix} Z_1(t) \\ N_1(t) \end{pmatrix} = \int d^3r \, g(x) \begin{pmatrix} J_{x,p}(\vec{r},t) \\ J_{x,n}(\vec{r},t) \end{pmatrix} = \begin{pmatrix} v_p(t) \\ v_n(t) \end{pmatrix}. \quad (6)$$

Mean values of the current densities of protons and neutrons along the collision direction are given by

$$J_{x,\alpha}(\vec{r},t) = \frac{\hbar}{m} \sum_{h\in\alpha} \text{Im}[\Phi_h^*(\vec{r},t) \nabla_x \Phi_h(\vec{r},t)], \qquad (7)$$

where the summation h runs over the occupied states originating both from the projectile and the target nuclei. The drift coefficients $v_p(t)$ and $v_n(t)$ denote the net proton and neutron currents across the window, respectively. In order to calculate the fluctuations of the proton and neutron numbers of the fragments we linearize the Langevin equation (2) around the mean values $v_p(t)$ and $v_n(t)$, and keep only the stochastic part of the currents to obtain

$$\frac{d}{dt} \begin{pmatrix} \delta Z_1^\lambda(t) \\ \delta N_1^\lambda(t) \end{pmatrix} = \begin{pmatrix} \delta v_p^\lambda(t) \\ \delta v_n^\lambda(t) \end{pmatrix}. \qquad (8)$$

The variances of neutron and proton distribution of projectile fragments are defined as $\sigma_{nn}^2(t) = \overline{(N_1^\lambda - N_1)^2}$ and $\sigma_{pp}^2(t) = \overline{(Z_1^\lambda - Z_1)^2}$. Multiplying both side of Eq. (8) by $N_1^\lambda - N_1$ and $Z_1^\lambda - Z_1$, and taking the ensemble averages, we find that the

proton and neutron variances are determined by

$$\frac{d}{dt}\sigma_{\alpha\alpha}^2(t) = 2D_{\alpha\alpha}(t), \tag{9}$$

where $D_{\alpha\alpha}(t)$ denote the diffusion coefficients of proton and neutron exchanges.

III. QUANTAL DIFFUSION COEFFICIENTS FOR NUCLEON EXCHANGE

The quantal expressions of the proton and neutron diffusion coefficients are determined by the correlation function of the stochastic part of the drift coefficients according to [38,39]

$$D_{\alpha\alpha}(t) = \int_0^t dt' \overline{\delta v_\alpha^\lambda(t)\delta v_\alpha^\lambda(t')}. \tag{10}$$

From Eq. (4), the stochastic parts of the drift coefficients are given by

$$\delta v_\alpha^\lambda(t) = \frac{\hbar}{m}\sum_{ij\in\alpha}\int d^3r g(x)\,\mathrm{Im}\big[\Phi_j^*(\vec{r},t)\nabla_x\Phi_i(\vec{r},t)\delta\rho_{ji}^\lambda\big]. \tag{11}$$

In determining the stochastic parts of the drift coefficients, we impose a physical constraint on the summations over single-particle sates. The transitions among single-particle states originating from the projectile or target nuclei do not contribute to the nucleon exchange mechanism. Therefore, in Eq. (11) we restrict the summation as follows: when the summation $i \in T$ runs over the states originating from target nucleus, the summation $j \in P$ runs over the states originating from the projectile, and vice versa. The main postulate of the SMF approach is that the stochastic part of the elements of the initial density matrix $\delta\rho_{ji}^\lambda$ have uncorrelated Gaussian distributions with zero mean values and second moments determined by [31]

$$\overline{\delta\rho_{ji}^\lambda\delta\rho_{i'j'}^\lambda} = \frac{1}{2}\delta_{ii'}\delta_{jj'}[n_i(1-n_j)+n_j(1-n_i)], \tag{12}$$

where n_j are the average occupation numbers of the single-particle states. Using this result, we can calculate the correlation functions of the stochastic part of the drift coefficients. At zero temperature, since the average occupation factor is 0 or 1, we find that the correlation functions are given by

$$\overline{\delta v_\alpha^\lambda(t)\delta v_\alpha^\lambda(t')} = \mathrm{Re}\Bigg[\sum_{p\in P,h\in T}A_{ph}^\alpha(t)A_{ph}^{*\alpha}(t')$$
$$+\sum_{p\in T,h\in P}A_{ph}^\alpha(t)A_{ph}^{*\alpha}(t')\Bigg]. \tag{13}$$

We note that, because of orthogonality, the particle states p and the hole states h must carry the same spin and isospin labels. The summation runs over the complete set of the particle and hole states of protons and neutrons. The matrix $A_{ph}^\alpha(t)$

is determined from the particle-hole states of the mean-field Hamiltonian,

$$A_{ph}^\alpha(t) = \frac{\hbar}{2m}\int d^3r g(x)\big[\Phi_p^{*\alpha}(\vec{r},t)\nabla_x\Phi_h^\alpha(\vec{r},t)$$
$$-\Phi_h^\alpha(\vec{r},t)\nabla_x\Phi_p^{*\alpha}(\vec{r},t)\big]. \tag{14}$$

With the help of partial integration we can express this matrix element as

$$A_{ph}^\alpha(t) = \frac{\hbar}{m}\int d^3r\,\Phi_p^{*\alpha}(\vec{r},t)g(x)\bigg[\nabla_x\Phi_h^\alpha(\vec{r},t)-\frac{x}{2\kappa^2}\Phi_h^\alpha(\vec{r},t)\bigg]. \tag{15}$$

In order to calculate the correlation function Eq. (13) directly, in addition the occupied hole states, we need to evolve a complete set of particle states. This is a very difficult task to accomplish. In a previous work, we carried out an approximate description of the correlation function by calculating it with a set of particle-hole states and increasing the volume of the particle-hole space step by step [40]. We observed that the convergence of such a calculation was very slow and required ever increasing computational time to proceed. Even the results obtained with sufficiently large particle-hole spaces did not compare favorably with the results of the semiclassical calculations.

Here, we introduce a different approach to evaluate the correlation function Eq. (13). In the first term of the right-hand side of Eq. (13), we add and subtract the hole contributions to give

$$\sum_{p\in P,h\in T}A_{ph}^\alpha(t)A_{ph}^{*\alpha}(t') = \sum_{a\in P,h\in T}A_{ah}^\alpha(t)A_{ah}^{*\alpha}(t')$$
$$-\sum_{h'\in P,h\in T}A_{h'h}^\alpha(t)A_{h'h}^{*\alpha}(t'). \tag{16}$$

Here, the summation a is over the complete set of states originating from the projectile. In the first term, we cannot use the closure relation to eliminate the complete set of single-particle states, because the wave functions are evaluated at different times. However, we note that the time-dependent single-particle wave functions during short time intervals exhibit nearly a diabatic behavior [41]. In another way of stating, that during short time intervals the nodal structure of time-dependent wave functions do not change appreciably. The most dramatic diabatic behavior of the time-dependent wave functions is apparent in the fission dynamics. The Hartree-Fock solutions force the system to follow the diabatic path, which prevents the system from breaking up into fragments. As a result of these observations, during the short time interval $\tau = t - t'$ evolutions, on the order of the correlation time, a diabatic approximation for the time-dependent wave functions can be done by shifting the time backward (or forward) according to

$$\Phi_a(\vec{r},t') \approx \Phi_a(\vec{r}-\vec{u}\tau,t), \tag{17}$$

where $\vec{u}$ denotes a suitable flow velocity of nucleons. Now, we can employ the closure relation

$$\sum_a \Phi_a^*(\vec{r}_1,t)\Phi_a(\vec{r}_2-\vec{u}\tau,t) = \delta(\vec{r}_1-\vec{r}_2+\vec{u}\tau), \tag{18}$$

where the summation a runs over the complete set of states originating from target or projectile, and the closure relation is valid for each set of the spin-isospin degrees of freedom. The flow velocity $\vec{u}(\vec{R}, T)$ may depend on the mean position $\vec{R} = (\vec{r}_1 + \vec{r}_2)/2$ and the mean time $T = (t + t')/2$. Employing the closure relation in the first term of the right-hand side of Eq. (16), we find

$$\sum_{a \in P, h \in T} A_{ah}^\alpha(t) A_{ah}^{*\alpha}(t') = \sum_{h \in T} \int d^3 r_1 d^3 r_2 \delta(\vec{r}_1 - \vec{r}_2 + \vec{u}_h \tau) \\ \times W_h^\alpha(\vec{r}_1, t) W_h^{*\alpha}(\vec{r}_2, t'). \quad (19)$$

In this manner the complete set of single-particle states is eliminated and the calculation of the expression is greatly simplified. In fact, in order to calculate this expression, we only need the hole states originating from target which are provided by the TDHF description. Rather than the mean flow velocity, we take local flow velocity $\vec{u}_h(\vec{R}, T)$ of each hole state across the window for each term in the summation. The local flow velocity of each wave function is specified by the usual expression of the current density divided by the particle density as given in Eq. (A6) in the Appendix. The quantity $W_h^\alpha(\vec{r}_1, t)$ becomes

$$W_h^\alpha(\vec{r}_1, t) = \frac{\hbar}{m} g(x_1) \Big[\nabla_1 \Phi_h^\alpha(\vec{r}_1, t) - \frac{x_1}{2\kappa^2} \Phi_h^\alpha(\vec{r}_1, t) \Big], \quad (20)$$

and $W_h^{*\alpha}(\vec{r}_2, t')$ is given by a similar expression. A detailed analysis of Eq. (19) under a certain approximation is presented in the Appendix. The result of this analysis as given by Eq. (16) is

$$\sum_{a \in P, h \in T} A_{ah}^\alpha(t) A_{ah}^{*\alpha}(t') = G(\tau) \int d^3 r \, \tilde{g}(x) J_{X,\alpha}^T(\vec{r}, t - \tau/2). \quad (21)$$

Here $J_{x,\alpha}^T(\vec{r}, t - \tau/2)$ represents the sum of the magnitude of the current densities due to wave functions originating from the target and it is given by Eq. (A17). The quantity $G(\tau)$ is the average value of the memory kernels $G_h(\tau)$ given by Eq. (A18). It is possible to carry out a similar analysis on the second term in the right side of Eq. (13), which yields,

$$\sum_{a \in T, h \in P} A_{ah}^\alpha(t) A_{ah}^{*\alpha}(t') = G(\tau) \int d^3 r \, \tilde{g}(x) J_{x,\alpha}^P(\vec{r}, t - \tau/2). \quad (22)$$

In a similar manner, $J_{x,\alpha}^P(\vec{r}, t - \tau/2)$ is determined by the sum of the magnitude of the current densities due to wave functions originating from projectile, and it is given by an equation similar to Eq. (A17). In Eqs. (21) and (22) we use lower-case $\vec{r}$ instead of a capital letter. As a result, the quantal expressions of the proton and neutron diffusion coefficients are given by

$$D_{\alpha\alpha}(t) = \int_0^t d\tau \, G(\tau) \int d^3 r \, \tilde{g}(x) \big[J_{x,\alpha}^T(\vec{r}, t - \tau/2) \\ + J_{x,\alpha}^P(\vec{r}, t - \tau/2) \big]$$

$$- \int_0^t d\tau \, \text{Re} \Bigg[\sum_{h' \in P, h \in T} A_{h'h}^\alpha(t) A_{h'h}^{*\alpha}(t - \tau) \\ + \sum_{h' \in T, h \in P} A_{h'h}^\alpha(t) A_{h'h}^{*\alpha}(t - \tau) \Bigg]. \quad (23)$$

To our knowledge, such a quantal expression for the nucleon diffusion coefficient in heavy-ion collisions is given here for the first time from a microscopic basis. There is a close analogy between the quantal expression and the classical diffusion coefficient in a random-walk problem [2,38,39]. The first line in the quantal expression gives the sum of the nucleon currents from the target-like fragment to the projectile-like fragment, which is integrated over the memory. This is analogous to the random walk problem, in which the diffusion coefficient is given by the sum of the rate for the forward and backward steps. The second line in the quantal diffusion expression stands for the Pauli blocking effect in the nucleon transfer mechanism, which does not have a classical counterpart. It is important to note that the quantal diffusion coefficients are entirely determined in terms of the occupied single-particle wave functions obtained from the TDHF solutions.

In the calculations carried out for the present study, we find that the average nucleon flow speed across the window between the colliding nuclei is around $u_x \approx 0.05c$. Using the expression $\tau_0 = \kappa/|u_x|$ given below Eq. (A18), with a dispersion $\kappa = 1.0$ fm, we find the memory time to be around $\tau_0 \approx 20$ fm/c. In the nuclear one-body dissipation mechanism, it is possible to estimate the memory time in terms of a typical nuclear radius and the Fermi speed as $\tau_0 \approx R/v_F$. If we take $R \approx 5.0$ fm and $v_F \approx 0.2c$, we find the same order of magnitude for the memory time, $\tau_0 \approx 25$ fm/c. Since it is much shorter than a typical interaction time of collisions at sub-barrier energies, $\tau_0 \ll 400$ fm/c, we find that the memory effect is not very effective in the nucleon exchange mechanism. We neglect the memory effect in the first line of the diffusion coefficient. The time integration of the memory kernel alone becomes

$$\tilde{G}(t) = \int_0^t d\tau \, G(\tau) = \int_0^t d\tau \, \frac{1}{\sqrt{4\pi}\tau_0} e^{-(\tau/2\tau_0)^2} \\ = \frac{1}{2} \text{erf}(t/2\tau_0). \quad (24)$$

Because of the same reason, the memory effect is not very effective in the Pauli blocking terms as well; however, in the calculations we keep the memory integrals in these terms.

IV. RESULTS OF CALCULATIONS

Employing the quantal diffusion mechanism described in the previous section, we investigate the nucleon exchange mechanism in central collisions of ^{28}O$+^{28}$O, ^{40}Ca$+^{40}$Ca, ^{48}Ca$+^{48}$Ca, and ^{56}Ni$+^{56}$Ni systems at bombarding energies slightly below the fusion barriers. Calculations were done in a three-dimensional Cartesian geometry with no symmetry assumptions [42] and using the Skyrme SLy4d interaction [43]. The three-dimensional Poisson equation for the Coulomb potential is solved by using fast Fourier transform techniques and the Slater approximation is used for the Coulomb

TABLE I. The fusion barriers and bombarding energies of the systems. The energies are given in MeV units.

System	Fusion barrier	Bombarding energy
$^{28}O + ^{28}O$	8.8	8.7
$^{40}Ca + ^{40}Ca$	53.2	52.7
$^{48}Ca + ^{48}Ca$	51.0	50.7
$^{56}Ni + ^{56}Ni$	100.7	100.0

exchange term. The box size used for all the calculations was chosen to be $60 \times 30 \times 30$ fm^3, with a mesh spacing of 1.0 fm in all directions. These values provide very accurate results due to the employment of sophisticated discretization techniques [44].

In Table I, we present the fusion barriers and the bombarding energies at which the calculations are carried out for these systems. During the reactions, colliding ions stick together with a visible neck for some time, and separate without forming a compound nucleus. Because of the symmetry, the mean values of proton and neutron numbers of the separated fragments remain equal to their initial values. However, proton and neutron numbers of the outgoing fragments have distributions around their mean values with variances determined by diffusion coefficients as

$$\sigma_{\alpha\alpha}^2(t) = 2 \int_0^t dt' D_{\alpha\alpha}(t'). \quad (25)$$

In a number of previous studies, we carried out calculations by employing the semiclassical approximation of the diffusion coefficient. We can obtain the semiclassical approximation of the diffusion coefficient by taking the Wigner transform of Eq. (23). In this manner, it is possible to express diffusion coefficients in terms of the phase-space distribution functions associated with single-particle wave functions originating from target and projectile nuclei. The semiclassical diffusion coefficients have a similar form that is familiar from the nucleon exchange transport model [2]. In order to avoid negative regions of the phase-space functions, an averaging procedure is carried out as outlined in [34–36]. Such an averaging procedure is particularly important for an accurate description of the Pauli blocking effects. In our presentation, we compare the quantal diffusion coefficients and the quantal variances for neutron and proton distributions of the outgoing fragments with their semiclassical approximation corresponding to the same reactions. The results of calculations of diffusion coefficients and variances for the systems investigated are presented in Figs. 1–4. The upper panels (a) of the figures show diffusion coefficients and the lower panels (b) illustrate variances as a function of times for the systems investigated. Solid lines and long-dashed lines indicate the quantal results for neutrons and protons, respectively. Similarly, short-dashed lines and dotted lines show the semiclassical results for neutrons and protons, respectively. The observed differences between the quantal and the semiclassical calculations originate from three different sources. The quantal calculations naturally include shell effects while in the semiclassical calculations the shell effects are washed out. In the mean-field description of the TDHF
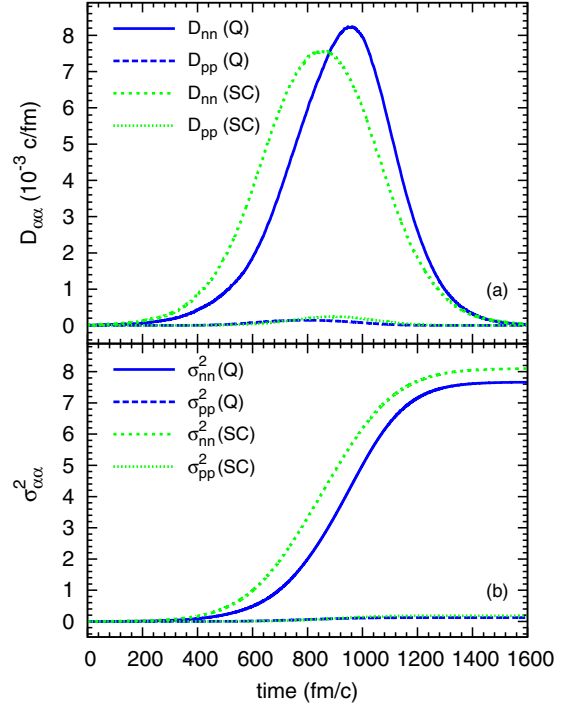
FIG. 1. Quantal and semiclassical neutron and proton diffusion coefficients (a) and corresponding variances (b) in central collisions of $^{28}O + ^{28}O$ at $E_{c.m.} = 8.7$ MeV.

approach the collective motion is treated in near classical approximation, but the single-particle motion is treated in a fully quantal manner. Therefore, in the quantal calculations, the barrier penetration of nucleons across the window is fully accounted for. On the other hand, in the semiclassical calculations only those nucleons above the barrier are allowed to cross the window. Particularly at low energies the barrier penetration in nucleon transfer can make a big difference for both protons and neutrons. In Table II, we list the asymptotic values of the proton and neutron variance for the systems investigated. We refer to the contribution by the part of the

TABLE II. Effect of Pauli blocking on fragment neutron and proton variances. The bombarding energies of all systems are given in Table I. Abbreviations Q and SC stand for quantal and semiclassical, respectively. PB stands for Pauli blocking and Δ is the difference between the variances with and without Pauli blocking.

		$\sigma_{nn}^2(t \to \infty)$			$\sigma_{pp}^2(t \to \infty)$		
		with PB	no PB	Δ_{nn}	with PB	no PB	Δ_{pp}
^{28}O	Q	7.66	9.57	−1.91	0.12	0.28	−0.16
	SC	8.10	8.72	−0.62	0.18	0.15	0.03
^{40}Ca	Q	0.67	1.51	−0.84	0.68	1.52	−0.84
	SC	1.03	1.11	−0.08	1.04	1.12	−0.08
^{48}Ca	Q	1.77	3.17	−1.4	0.54	1.21	−0.67
	SC	1.97	2.35	−0.38	0.70	0.72	−0.02
^{56}Ni	Q	3.46	5.44	−1.98	3.23	5.25	−2.02
	SC	3.98	4.20	−0.22	3.84	4.09	−0.25

variances arising from the first line in the diffusion coefficient in Eq. (23) as the direct term, and we refer to the term due to the second line as the blocking term.

We observe by comparing the second column for neutrons and the second column for protons in Table II that the direct contributions in the variances in the quantal calculations are larger than the semiclassical results (mainly as a result of the barrier penetration). The third important difference between the quantal and the semiclassical results arises from the Pauli blocking terms in the diffusion coefficient. In the quantal calculations the Pauli blocking terms are calculated exactly. On the other hand, the Pauli blocking effects in the semiclassical limit are treated in an approximate manner. By comparing the third column for neutrons and the third column for protons in Table II, we notice large differences in the magnitude of the Pauli blocking terms between the quantal and the semiclassical calculations. In fact, for some situations the averaging procedure to eliminate the negative regions of the phase-space functions may not work very well; consequently the sign of the Pauli blocking terms can become positive rather than negative. Because of these different effects, the asymptotic values of the proton and neutron variances for the quantal calculations may be smaller or larger that the result of the semiclassical calculations. Even the small differences in the variances can have a large effect on the production of rare neutron-rich isotopes by the diffusion mechanism. It is important to note, not only are the quantal diffusion calculations more accurate, but also the quantal calculations take less numerical effort than their semiclassical counterparts.

From Figs. 1–4, we observe that in the collisions of neutron-rich nuclei, $^{28}O + ^{28}O$ and $^{48}Ca + ^{48}Ca$, the neutron variances are larger than the proton variances, while in the collisions of $^{40}Ca + ^{40}Ca$ and $^{56}Ni + ^{56}Ni$ nuclei the variances are nearly equal. In neutron-rich nuclei, due to the halo structure, the tail of neutron distribution extends further outward, while the proton distribution, particularly in the ^{28}O nucleus, behaves like an inert core. This structure effect leads to more neutron exchanges during the collision. Hence the outgoing fragments have broader neutron number distributions. We also notice from Figs. 2 and 3 that the quantal variances in the system $^{40}Ca + ^{40}Ca$ are nearly 40% smaller than the semiclassical variances, while in the $^{48}Ca + ^{48}Ca$ system the quantal and the semiclassical variances are nearly the same. We believe that this difference appears partly as a result of the more compact quantal structure of ^{40}Ca than that of the neutron-rich isotope ^{48}Ca. Also, the Pauli blocking effect is partly responsible for this behavior: As seen from Table II, the Pauli blocking in the $^{40}Ca + ^{40}Ca$ system is poorly described in the semiclassical approximation for both proton and neutron transfers, leading to larger variances in the semiclassical calculations. Unfortunately, we are not able to compare the present calculations with data. However, currently we are investigating quantal diffusion mechanisms in heavy-ion collisions with finite impact parameters. This study will allow us to analyze experimental data on multinucleon transfer processes in deep-inelastic collisions and quasifission reactions. We should mention that there are a number of other investigations of the dispersion of fragment mass distribution in nuclear reactions [45,46] by employing the variational approach of
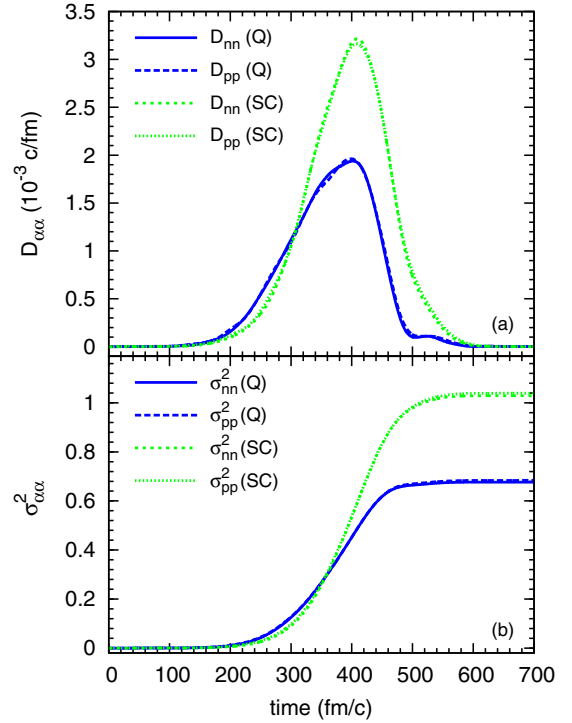

FIG. 2. Quantal and semi classical neutron and proton diffusion coefficients (a) and corresponding variances (b) in central collisions of $^{40}Ca + ^{40}Ca$ at $E_{c.m.} = 52.7$ MeV.
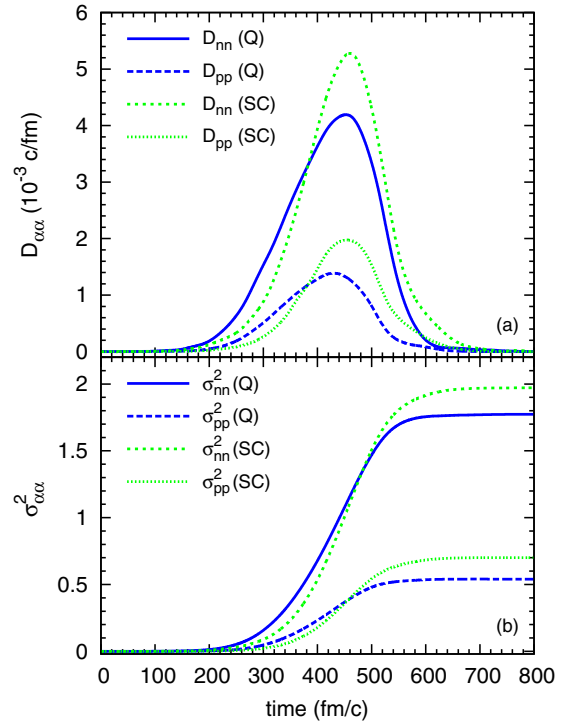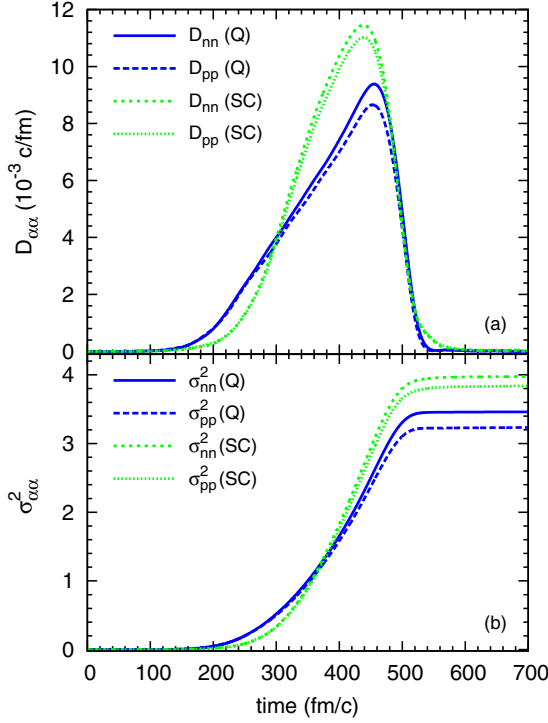

FIG. 3. Quantal and semiclassical neutron and proton diffusion coefficients (a) and corresponding variances (b) in central collisions of $^{48}Ca + ^{48}Ca$ at $E_{c.m.} = 50.7$ MeV.

FIG. 4. Quantal and semiclassical neutron and proton diffusion coefficients (a) and corresponding variances (b) in central collisions of ^{56}Ni $+^{56}$Ni at $E_{c.m.} = 100$ MeV.

Balian-Veneroni [47] and number projection techniques [48]. We should note also that, as demonstrated in [31], it is possible to recover the dispersion formula of Balian-Veneroni, in the special case of small amplitude fluctuations from the SMF approach.

V. CONCLUSIONS

In the standard mean-field approach, the collective motion is treated semiclassically. The SMF approach improves the standard description by incorporating thermal and quantal fluctuations in the initial states. In this manner, the SMF approach provides an approximate description of the quantal fluctuation dynamics of collective motion at low energies where collisional dissipation is not very effective. Under certain circumstances, the fluctuation dynamics can be approximately described in terms of transport coefficients associated with the collective variables. In this work, we consider central collisions of symmetric nuclei below the fusion barrier and study the nucleon exchange mechanism in the SMF approach. Since binary structure is maintained during the collision, it is possible to determine macroscopic variables by a geometric projection procedure. The SMF approachgives rise to a Langevin description for evolution of macroscopic variables. In this work, we consider the nucleon exchange mechanism in central collisions of symmetric nuclei and extract quantal expression for the diffusion coefficients of proton and neutron exchanges. We carry out calculations of proton and neutron variances in central collisions of ^{28}O $+^{28}$O, ^{40}Ca $+^{40}$Ca, ^{48}Ca $+^{48}$Ca, and ^{56}Ni $+^{56}$Ni systems at bombarding energies

slightly below the fusion barriers, and compare the quantal results with the corresponding semiclassical calculations. There are important differences between the quantal and the semiclassical calculations due to mainly three different mechanisms. First of all the quantal calculations involve shell effects, while the shell effects are smoothed out in the semiclassical calculations. The barrier penetration of protons and neutrons during the transfer across the window is properly taken into account in the quantal description. In the semiclassical calculations, nucleon transfers are totally blocked below the barrier of the mean-field potential. More importantly, in the quantal description, the Pauli blocking effect in the transfer mechanism is taken into account exactly, while in the semiclassical calculations it is taken into account in an approximate manner. The quantal calculations provide a more accurate description of the diffusion coefficients, but surprisingly they require less numerical effort than the semiclassical calculations.

APPENDIX: ANALYSIS OF THE CLOSURE RELATION

We rewrite Eq. (16) as

$$\sum_{a \in P, h \in T} A_{ah}^{\alpha}(t) A_{ah}^{*\alpha}(t') = \sum_{h \in T} \int d^3 R \, d^3 r \, \delta(\vec{r} + \vec{u}_h \tau)$$
$$\times W_h^{\alpha}(\vec{r}_1, t) W_h^{*\alpha}(\vec{r}_2, t'), \quad \text{(A1)}$$

where we introduce the coordinate transformation

$$\vec{R} = (\vec{r}_1 + \vec{r}_2)/2, \quad \vec{r} = \vec{r}_1 - \vec{r}_2, \quad \text{(A2)}$$

and its reverse as

$$\vec{r}_1 = \vec{R} + \vec{r}/2, \quad \vec{r}_2 = \vec{R} - \vec{r}/2. \quad \text{(A3)}$$

For clarity, we present quantities $W_h^{\alpha}(\vec{r}_1, t)$ and $W_h^{*\alpha}(\vec{r}_2, t')$ here again:

$$W_h^{\alpha}(\vec{r}_1, t') = \frac{\hbar}{m} g\left(X + \frac{x}{2}\right)\left[\nabla_X i_h^{\alpha}\left(\vec{R} + \frac{\vec{r}}{2}, t'\right)\right.$$
$$\left. - \frac{X + x/2}{2\kappa^2}\Phi_h^{\alpha}\left(\vec{R} + \frac{\vec{r}}{2}, t'\right)\right] \quad \text{(A4)}$$

and

$$W_h^{*\alpha}(\vec{r}_2, t') = \frac{\hbar}{m} g\left(X - \frac{x}{2}\right)\left[\nabla_X \Phi_h^{*\alpha}\left(\vec{R} - \frac{\vec{r}}{2}, t'\right)\right.$$
$$\left. - \frac{X - x/2}{2\kappa^2}\Phi_h^{*\alpha}\left(\vec{R} - \frac{\vec{r}}{2}, t'\right)\right]. \quad \text{(A5)}$$

The local flow velocity of the wave function $\Phi_h^\alpha(\vec{R},T)$ is calculated in the standard manner,

$$\vec{u}_h^\alpha(\vec{R},T) = \frac{\hbar}{m}\frac{1}{|\Phi_h^\alpha(\vec{R},T)|^2}\text{Im}\big[\Phi_h^{*\alpha}(\vec{R},T)\vec{\nabla}\Phi_h^\alpha(\vec{R},T)\big], \quad \text{(A6)}$$

with $T = (t+t')/2 = t - \tau/2$. Because of the delta function in the integrand of Eq. (A1), we make the substitution $\vec{r} = -\vec{u}_h^\alpha(\vec{R},T)\tau$ in the wave functions and introduce the backward diabatic shift to obtain

$$\Phi_h^\alpha(\vec{R}+\vec{r}/2,t) = \Phi_h^\alpha(\vec{R}-\vec{u}_h^\alpha\tau/2,t) \approx \Phi_h^\alpha(\vec{R},T) \quad \text{(A7)}$$

and

$$\Phi_h^\alpha(\vec{R}-\vec{r}/2,t') = \Phi_h^\alpha(\vec{R}+\vec{u}_h^\alpha\tau/2,t') \approx \Phi_h^\alpha(\vec{R},T). \quad \text{(A8)}$$

After making this substitution, Eq. (A1) becomes

$$\frac{m^2}{\hbar^2}\sum_{a\in P, h\in T} A_{ah}^\alpha(t)A_{ah}^{*\alpha}(t')$$
$$= \sum_{h\in T}\int d^3R\,\tilde{g}(X)\frac{G_h(\tau)}{|u_X^h(\vec{R},T)|}\bigg[\big|\nabla_X\Phi_h^\alpha(\vec{R},T)\big|^2$$
$$- \frac{X}{2\kappa^2}\nabla_X\big(|\Phi_h^\alpha(\vec{R},T)|^2\big) + \frac{X^2-\big(u_X^h\tau/2\big)^2}{4\kappa^4}\big|\Phi_h^\alpha(\vec{R},T)\big|^2\bigg]. \quad \text{(A9)}$$

In this expression $\tilde{g}(X)$ is sharp as Gaussian smoothing function centered on the window with a dispersion $\kappa = 0.5$ fm,

$$\tilde{g}(X) = \frac{1}{\sqrt{\pi}\kappa}\exp[-(X/\kappa)^2], \quad \text{(A10)}$$

and $G_h(\tau)$ indicates the memory kernel,

$$G_h(\tau) = \frac{1}{\sqrt{4\pi}}\frac{1}{\tau_o^h}\exp\big[-\big(\tau/2\tau_o^h\big)^2\big], \quad \text{(A11)}$$

with the memory time $\tau_0^h = \kappa/|u_h^h|$. Due to the fact that $\tilde{g}(X)$ is centered at $X = 0$, the second term in Eq. (A9) is nearly zero. In the third term, after carrying out an average over the memory, the factor in the middle becomes

$$X^2 - \big(u_x^h\tau/2\big)^2 \to X^2 - (\kappa/2)^2. \quad \text{(A12)}$$

Since the Gaussian $\tilde{g}(X)$ is sharply peaked around $X = 0$ with a variance $(\kappa/2)^2$, the third term in Eq. (A9) is expected to

be very small, as well. Neglecting the second and third terms, Eq. (A9) becomes

$$\frac{m^2}{\hbar^2}\sum_{a\in P, h\in T} A_{ah}^\alpha(t)A_{ah}^{*\alpha}(t')$$
$$= \sum_{h\in T}\int d^3R\,\tilde{g}(X)\frac{G_h(\tau)}{|u_X^h(\vec{R},T)|}\big|\nabla_X\Phi_h^\alpha(\vec{R},T)\big|^2. \quad \text{(A13)}$$

Furthermore, it is useful to express the wave function in terms of its magnitude and its phase as [49]

$$\Phi_h^\alpha(\vec{R},T) = \big|\Phi_h^\alpha(\vec{R},T)\big|\exp\big[iQ_h^\alpha(\vec{R},T)\big]. \quad \text{(A14)}$$

The phase factor $Q_h^\alpha(\vec{R},T)$ behaves as the velocity potential of the flow velocity of the wave. Using the definition given by Eq. (A6), we observe that the flow velocity is given by $\vec{u}_h^\alpha(\vec{R},T) = (\hbar/m)\vec{\nabla}Q_h^\alpha(\vec{R},T)$. In the vicinity of the window, in the perpendicular direction, the phase varies faster than the magnitude of the wave function. Neglecting the small variation of the magnitude $|\Phi_h(\vec{R},T)|$, we can express the gradient of the wave function in Eq. (A13) as

$$\nabla_X\Phi_h^\alpha(\vec{R},T) \approx i\Phi_h^\alpha(\vec{R},T)\nabla_X Q_h^\alpha(\vec{R},T). \quad \text{(A15)}$$

As a result, Eq. (A1) becomes

$$\sum_{a\in P, h\in T} A_{ah}^\alpha(t)A_{ah}^{*\alpha}(t')$$
$$= G(\tau)\int d^3R\,\tilde{g}(X)J_{X,\alpha}^T(\vec{R},t-\tau/2). \quad \text{(A16)}$$

Here, the quantity $J_{X,\alpha}^T(\vec{R},t-\tau/2)$ in the integrand represents the sum of the magnitude of the current densities due to wave functions originating from the target:

$$J_{X,\alpha}^T(\vec{R},t-\tau/2)$$
$$= \frac{\hbar}{m}\sum_{h\in T}|\text{Im}[\Phi_h^*(\vec{R},t-\tau/2)\nabla_X\Phi_h(\vec{R},t-\tau/2)]|. \quad \text{(A17)}$$

In obtaining Eq. (A16), we introduced a further approximation by replacing the individual memory kernels $G_h(\tau)$ by its average value taken over the hole states,

$$G(\tau) = \frac{1}{\sqrt{4\pi}}\frac{1}{\tau_0}\exp[-(\tau/2\tau_0)^2], \quad \text{(A18)}$$

with the memory time determined by the average speed u_X as $\tau_0 = \kappa/|u_X|$.

[1] S. Ayik, B. Schürmann, and W. Nörenberg, Z. Phys. A **279**, 145 (1976).

[2] J. Randrup, Nucl. Phys. A **327**, 490 (1979).

[3] A. C. Merchant and W. Nörenberg, Z. Phys. A **308**, 315 (1982).

[4] W. U. Schröder, J. R. Huizenga, and J. Randrup, Phys. Lett. B **98**, 355 (1981).

[5] W. Loveland, Phys. Rev. C **76**, 014612 (2007).

[6] G. Fazio, G. Giardina, G. Mandaglio, R. Ruggeri, A. I. Muminov, A. K. Nasirov, Yu. Ts. Oganessian, A. G. Popeko, R. N.

Sagaidak, A. V. Yeremin, S. Hofmann, F. Hanappe, and C. Stodel, Phys. Rev. C **72**, 064614 (2005).

[7] G. G. Adamian, N. V. Antonenko, and W. Scheid, Phys. Rev. C **68**, 034601 (2003).

[8] G. G. Adamian, N. V. Antonenko, and W. Scheid, Eur. Phys. J. A **41**, 235 (2009).

[9] A. K. Nasirov, G. Giardina, G. Mandaglio, M. Manganaro, F. Hanappe, S. Heinz, S. Hofmann, A. I. Muminov, and W. Scheid, Phys. Rev. C **79**, 024606 (2009).

[10] Zhao-Qing Feng, Gen-Ming Jin, Jun-Qing Li, and Werner Scheid, Nucl. Phys. A **816**, 33 (2009).

[11] A. Diaz Torres, G. G. Adamian, N. V. Antonenko, and W. Scheid, Nucl. Phys. A **679**, 410 (2001).

[12] V. I. Zagrebaev, Phys. Rev. C **64**, 034606 (2001).

[13] A. Diaz-Torres, G. G. Adamian, N. V. Antonenko, and W. Scheid, Phys. Rev. C **64**, 024604 (2001).

[14] Y. Aritomo and M. Ohta, Nucl. Phys. A **744**, 3 (2004).

[15] V. Zagrebaev and W. Greiner, J. Phys. G **31**, 825 (2005).

[16] A. Diaz-Torres, Phys. Rev. C **74**, 064601 (2006).

[17] J. W. Negele, Rev. Mod. Phys. **54**, 913 (1982).

[18] C. Simenel, Eur. Phys. J. A **48**, 152 (2012).

[19] C. Rizzo, V. Baran, M. Colonna, A. Corsi, and M. Di Toro, Phys. Rev. C **83**, 014604 (2011).

[20] C.-C. Sahm, H.-G. Clerc, K.-H. Schmidt, W. Reisdorf, P. Armbruster, F. P. Heßberger, J. G. Keller, G. Münzenberg, and D. Vermeulen, Z. Phys. A **319**, 113 (1984).

[21] K.-H. Schmidt and W. Morawek, Rep. Prog. Phys. **54**, 949 (1991).

[22] V. Zagrebaev and W. Greiner, J. Phys. G **34**, 2265 (2007).

[23] Y. Aritomo, Phys. Rev. C **80**, 064604 (2009).

[24] A. Wakhle, C. Simenel, D. J. Hinde, M. Dasgupta, M. Evers, D. H. Luong, R. du Rietz, and E. Williams, Phys. Rev. Lett. **113**, 182502 (2014).

[25] V. E. Oberacker, A. S. Umar, and C. Simenel, Phys. Rev. C **90**, 054605 (2014).

[26] A. S. Umar, V. E. Oberacker, and C. Simenel, Phys. Rev. C **92**, 024621 (2015).

[27] A. S. Umar and V. E. Oberacker, Nucl. Phys. A **944**, 238 (2015).

[28] M. Tohyama and A. S. Umar, Phys. Lett. B **549**, 72 (2002).

[29] C. Simenel, Phys. Rev. Lett. **106**, 112502 (2011).

[30] D. Lacroix and S. Ayik, Eur. Phys. J. A **50**, 95 (2014).

[31] S. Ayik, Phys. Lett. B **658**, 174 (2008).

[32] S. Ayik, K. Washiyama, and D. Lacroix, Phys. Rev. C **79**, 054606 (2009).

[33] K. Washiyama, S. Ayik, and D. Lacroix, Phys. Rev. C **80**, 031602 (2009).

[34] B. Yilmaz, S. Ayik, D. Lacroix, and K. Washiyama, Phys. Rev. C **83**, 064615 (2011).

[35] B. Yilmaz, S. Ayik, D. Lacroix, and O. Yilmaz, Phys. Rev. C **90**, 024613 (2014).

[36] S. Ayik, B. Yilmaz, and O. Yilmaz, Phys. Rev. C **92**, 064615 (2015).

[37] D. Lacroix, S. Ayik, and B. Yilmaz, Phys. Rev. C **85**, 041602 (2012).

[38] C. W. Gardiner, *Quantum Noise* (Springer-Verlag, Berlin, 1991).

[39] U. Weiss, *Quantum Dissipative Systems*, 2nd ed. (World Scientific, Singapore, 1999).

[40] S. Ayik, O. Yilmaz, B. Yilmaz, A. S. Umar, A. Gokalp, G. Turan, and D. Lacroix, Phys. Rev. C **91**, 054601 (2015).

[41] W. Nörenberg, Phys. Lett. B **104**, 107 (1981).

[42] A. S. Umar and V. E. Oberacker, Phys. Rev. C **73**, 054607 (2006).

[43] K.-H. Kim, T. Otsuka, and P. Bonche, J. Phys. G **23**, 1267 (1997).

[44] A. S. Umar, M. R. Strayer, J. S. Wu, D. J. Dean, and M. C. Güçlü, Phys. Rev. C **44**, 2512 (1991).

[45] J. B. Marston and S. E. Koonin, Phys. Rev. Lett. **54**, 1139 (1985).

[46] J. M. A. Broomfield and P. D. Stevenson, J. Phys. G **35**, 095102 (2008).

[47] R. Balian and M. Vénéroni, Ann. Phys. (N.Y.) **164**, 334 (1985).

[48] C. Simenel, Phys. Rev. Lett. **105**, 192701 (2010).

[49] K. Gottfried, *Quantum Mechanics* (W. A. Benjamin, New York, 1966).